Comparison Between Equivalent-Circuit and Black-Box Non-Linear Models for Microwave Electron Devices

A. Raffo[1-2], J.A. Lonac[3], S. Menghi[3], R. Cignani[1-4]

[1]Department of Engineering, University of Ferrara, Via Saragat 1, 44100 Ferrara, Italy.
e-mail: araffo@ing.unife.it , rcignani@ing.unife.it .
[2]CoRiTeL, Via Anagnina 203, 00040 Morena (Rome), Italy.
[3]Department of Electronics, University of Bologna, Viale Risorgimento 2, 40136 Bologna, Italy.
e-mail: jalonac@deis.unibo.it .
[4]MEC Srl – Viale Pepoli 3/2 - 40126 Bologna, Italy.

***Abstract* — Black-box and Equivalent-circuit electron device models present different advantages. The first ones are independent from process and device technology (i.e, GaAs, InP, GaN). In the other side the black-box model extraction procedure could not be changed and modified, thus a "post-tune" procedure is not possible. On the contrary, equivalent circuits are strongly technology dependent, though they are more flexible in the identification procedure. In fact an "optimization" of the extracted model parameters is possible following a trade-off with measured data over a large set of bias conditions and frequencies. In this paper two device models, which represent the two categories, will be compared pointing out the differences in the extraction procedures and in the achievable accuracy under small-signal and large-signal operating conditions.**

INTRODUCTION

It is well known that Black-box and Equivalent-circuit electron device models present different advantages. In particular, black-box models are based on a general mathematical formulation and adopt some simplifying hypothesis that make the mathematical treatment and model identification feasible. These models have the great advantage of being independent from the process and the device technology (i.e GaAs, InP, GaN) but the main hypotheses are usually related only to the general and basic properties of the electron devices. Unfortunately, black-box models are scarcely flexible during the extraction procedure; more precisely, if the model accuracy is not satisfying, there is no way to "post-tune" any element and the entire extraction procedure must be repeated. On the contrary, equivalent circuits are strictly related to the physic of the device. This model category is strongly technology dependent even though is more flexible during the identification phase. After having identified all the model parameters it is possible to perform an optimization procedure with the aim of fitting measured data and carrying out the best trade-off over a large set of bias conditions, frequencies and non-linear working conditions.

In this paper the black-box NDC model (described in section I) and the equivalent circuit EEFET3 model (described in section II), will be compared pointing out the differences in the extraction procedures and the small- and large-signal prediction capabilities.

I. THE NDC MODEL

The time-domain current/voltage relationship of a single port electron device can be expressed as:

$$i(t) = \lim_{T_M \to +\infty} \Psi\left| v(t-\tau), V_0, \vartheta_0 \right|_{\tau=0}^{T_M} \qquad (1)$$

where $\Psi\left|\cdot\right|$ is a suitable nonlinear functional, which represents the nonlinear dependence of the device current i at the generic instant t on the present and past values of the applied voltage $v(t-\tau)$ over a virtually infinite memory time interval T_M. The dependence of the current $i(t)$ on the average voltage component V_0 and average channel temperature ϑ_0 has been introduced to describe in a simplified way the low-frequency dispersive phenomena due to "traps" and thermal effects. This allows to separate the long lasting memory of the LF-phenomena from the relatively "short" memory dynamics associated with all the other charge storage phenomena within the device. In fact, the main simplification which leads to the NDC model derives from the basic hypothesis that, apart from low-frequency dispersion and linear parasitic elements which are usually modeled separately, all the other device dynamics is limited to a memory time T_M which is not only practically finite, but also relatively short (i.e., much shorter than the period of the typical operating signals). The validity of such an hypothesis is well verified for the intrinsic device (i.e. after de-embedding from parasitic elements) as confirmed by accurate numerical device simulations and experimental results [1-2].

When the short memory condition is satisfied, so that a small, finite T_M can be used in (1) without introducing any relevant memory truncation error, the device dynamics can be more conveniently described in terms of "dynamic voltage deviations" $e(t, \tau)$ defined as the difference the past value v(t-τ) of the applied voltage

with respect to the present value *v(t)*. In particular (1) can be linearised and described in terms of a linear convolution with respect to *e(t, τ)*:

$$i(t) = F^{LF}\left[v(t), V_0, \vartheta_0\right] + \int_0^{T_M} g\left[v(t), \tau\right] e(t, \tau)\, d\tau \tag{2}$$

Equation (2) represents a finite memory nonlinear model which correctly describes the behavior of very different electron devices; in fact suitable values of T_M can be found for which the errors due to both memory truncation and linearization with respect to the dynamic deviations are small enough. To make model extraction and implementation feasible, the memory time of the nonlinear intrinsic device is divided into a suitable number N_D of intervals of width $\Delta\tau$. This allows for a formulation of the model where the dynamic deviation is a function of a finite number of points in the τ domain, while the voltage-controlled pulse response is expressed by means of a p index which "discretises" the convolution integral by a finite summation:

$$\begin{aligned} i(t) = \; & F^{LF}\left[v(t), V_0, \vartheta_0\right] + \\ & \sum_{p=1}^{N_D} g_p\left[v(t)\right] \cdot \left[v(t - p\Delta\tau) - v(t)\right] + \Delta i_{par}(t) \end{aligned} \tag{3}$$

The term $F_{LF}[v(t); V_0, \vartheta_0]$ in (3) describes the device behavior at DC and low-frequency operation. Different approaches were developed to define the F_{LF} characteristic [3-4]. The second term in (3) represents a discretised purely-dynamic single-fold convolution integral between voltage deviations and the "pulse response function" $g[v(t), \tau]$ nonlinearly-controlled by the instantaneous applied voltage. This term accounts for purely-dynamic nonlinear phenomena which are important at high frequencies. An additional current contribution $\Delta i_{par}(t)$ has also been included in (3) in order to account for additional parallel parasitic elements, as shown in Fig.1 for the two-port case. Equation (3) represents the final formulation of the Nonlinear Discrete Convolution model which can be efficiently applied to a large variety of electron devices to obtain accurate predictions under large-signal operating conditions, in fact no hypothesis has been made on the device technology (HBT, FET) or material.

The NDC model can be easily identified starting from conventional DC and bias dependent small-signal parameter measurements [1-2]. In particular the extraction program simply asks the user to define the extrinsic parasitic network to de-embed the measured data, the memory time T_M for the specific device and the number N_D of intervals of width $\Delta\tau = T_M / N_D$ to be considered (three intervals represent a good compromise between model accuracy and model implementation complexity).

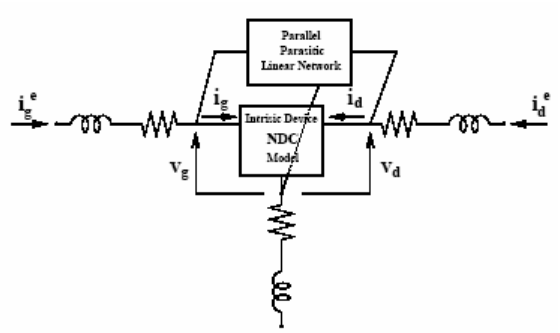

Fig. 1. The equivalent scheme of the NDC model.

II. THE EEFET3/EEHEMT1 IC-CAP MODEL

The Agilent IC-CAP modeling system provides a guided procedure to measure semiconductor devices and to exploit the resulting data for model extraction. Furthermore, IC-CAP provides a complete set of library model types and extraction procedures for a wide set of devices (HBT, PHEMT, BJT, MOSFET, MESFET).

For HEMT type devices IC-CAP offers the EEFET3/EEHEMT1 model [5-6], which is an empirical analytic model developed for GaAs FETs and HEMTs. This model, whose equivalent circuit scheme is shown in Fig. 2, includes features for self-heating, charge modeling, high frequency dispersion and breakdown.

The extraction procedure is divided in measurement setups. Each measurement setup defines a set of measures that allow for the determination of data useful for the next setups and specific model parameters extraction. Successive setups depend on previous setups, therefore the order in which the setups are performed must be respected. The extraction procedure begins with the identification of the parasitic elements; since the successive setups depend on the parasitics previously extracted the parasitic identification is a key point for model extraction.

Each setup has a set of dedicated functions (namely "transforms" in the IC-CAP environment) that allow for the extraction of each parameter used to describe elements of the equivalent circuit model. The setups also offer the possibility to optimize the extracted parameters; so it is possible to tune a specific equivalent circuit component without affecting the rest of the model, this "independent tunability" is not offered by black-box models and therefore the model must be re-extracted completely if it does not fit the desired measured characteristics.

Fig. 3 gives an example of the flexibility of equivalent circuit models. This figure shows the gate diode characteristic as resulting from the parameter extraction procedure and the same line after an optimization performed with the aim to perfectly match gate diode characteristic of the model with the measurements. As it can be seen the guided extraction procedure offered by IC-CAP allows optimizing the parameters correspondent to the gate diode in order to fit the measured characteristic independently from other equivalent circuit parameters. This independent tunability is available for almost all the extraction setups, making it possible to repeat a model parameter extraction without changing the

remaining model parameters determined in the previous setups.

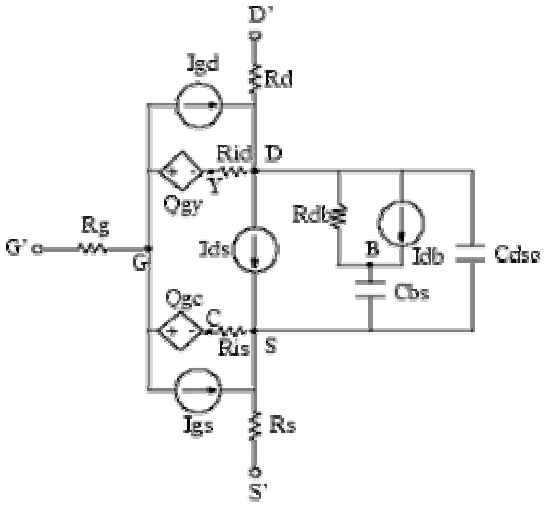

Fig. 2. The equivalent circuit of the EEHEMT1 model.

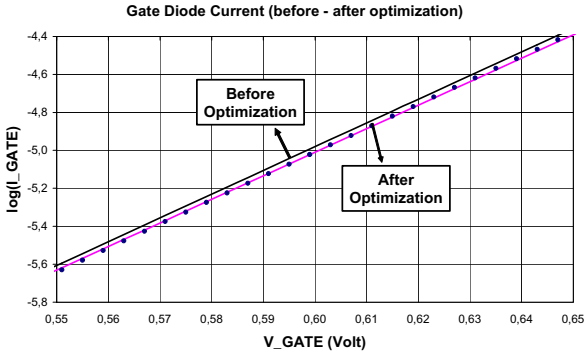

Fig. 3. Simulated and measured (dot line) gate-diode current versus gate-source voltage before and after the optimization.

III. Experimental Results

The identification procedures have been carried out for a GaAs PHEMT with a gate length of 0.25 µm and a total periphery of 200 µm (4*50 µm). Small signal and large signal measurements, achieved on this device, have been compared with the simulated performances estimated by the two different models.

In order to test the small-signal prediction capabilities of the models, measurements of the pHEMT S-parameters were carried out for different biases at 10 GHz and compared with the NDC and EEHEMT1 model predictions. Corresponding results are shown in Fig. 4 and in Fig. 5 for the S21-parameter. As can be seen, the NDC model predictions are more accurate also considering the capability of reproducing concavity and convexity of the bias-dependent measured small-signal parameters. Analogous results have been obtained for the other small-signal parameters.

Large-signal prediction capabilities of the two models have been tested by Harmonic Distortion measurements carried out at 5 GHz and biasing the device in class-A operation mode. In Fig. 6, the measured transducer power gain, at different input power levels, is compared with the results carried out by the two models. It is possible to notice a good agreement between the NDC predictions and the measurements.

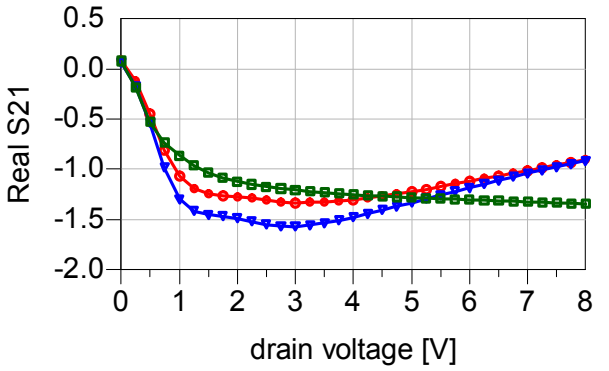

Fig. 4. – Extrinsic real part of the S21 parameter at 10 GHz for the 0.25 µm GaAs PHEMT considered at different drain biases and V_{g0}= -0.6V. Measurements (circles) versus predictions based on EEHEMT1 (squares) and NDC (triangles) models.

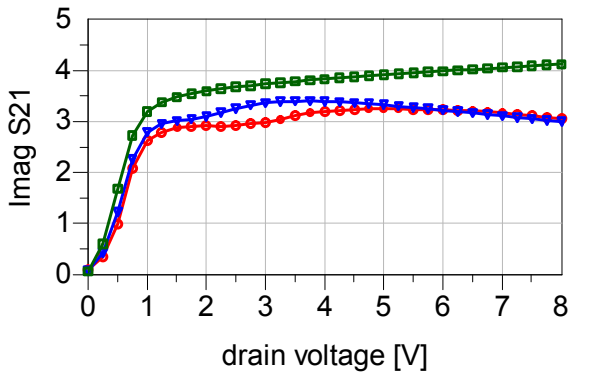

Fig. 5. – Extrinsic imaginary part of the S21 parameter at 10 GHz for the 0.25 µm GaAs PHEMT considered at different drain biases and Vg0= -0.6V. Measurements (circles) versus predictions based on EEHEMT1 (squares) and NDC (triangles) models.

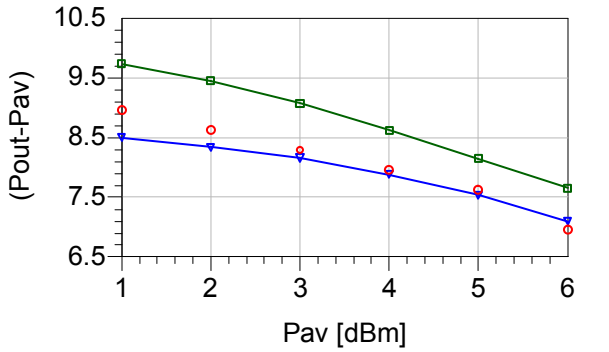

Fig. 6. – Transducer power gain. Measurements (circles) versus predictions based on EEHEMT1 (squares) and NDC (triangles) models.

In order to further evaluate the nonlinear high-frequency prediction accuracy of the models, measurements of the third-order intermodulation product (interferer) to carrier ratio (I/C) were carried out at the frequency of 4 GHz (two tone displacement: 50MHz; class-A operation: VGS=-0.55V, VDS=5V). Simulation and measurement results are shown in Fig. 7 as a function of the output power. As can be seen the NDC

model is in perfect agreement with measurements at the lower levels of output power, though some little differences could be observed for an output power major than 4 dBm. On the contrary the EEHEMT model shows a very good fitting only for high output power levels.

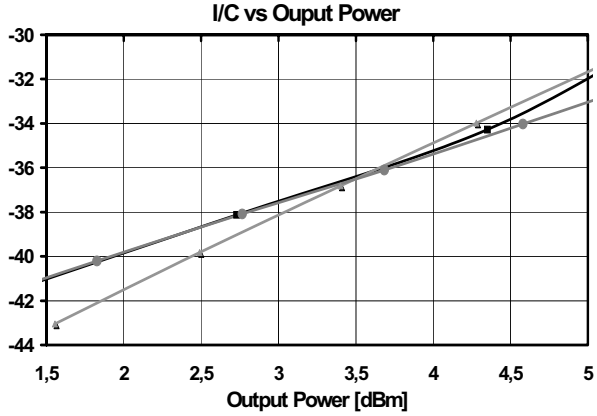

Fig. 7. – Third-order intermodulation product (Interfer) to Carrier ratio versus output power (Single Carrier Level) Measurements (Black line with squares) are compared to prediction based on the NDC model (Gray line with triangles) and EEHEMT1 (Gray line with circles) models.

VI. Conclusion

In this paper has been proposed a comparison between two different models based respectively on black-box and equivalent circuit approaches.

After a brief overview on model identification and extraction procedures, where the advantages and the disadvantages of the two different models have been pointed out, different comparisons with measurements have been proposed.

The simulation results of the two models under small-signal condition have been compared with S-parameters measurements. Moreover measurements under large-signal conditions (transducer power gain and intermodulation product) have been compared with the same ones achieved in the ADS environments utilizing the black-box model and the equivalent circuit one.

In particular it has been observed that the two models show the same prediction capability under large-signal operating conditions, while a slight better prediction accuracy is presented by the black-box model under small-signal operating conditions.

Acknowledgement

This work was partly funded by the Italian Ministry of Instruction, University and Research within the project "Modelli di dispositivi elettronici per il progetto di circuiti integrati monolitici a microonde ed onde millimetriche per collegamenti radio di nuova generazione ad elevate prestazioni".

References

[1] F.Filicori, A.Santarelli, P.Traverso, G.Vannini: “Electron device model based on Nonlinear Discrete Convolution for large-signal circuit analysis using commercial CAD packages”, *Proc. of GAAS'99, Gallium Arsenide Applications Symposium*, Munich, Germany, pp. 225-230,October 4-5, 1999.

[2] A. Costantini, R.P.Paganelli et al: “Accurate prediction of PHEMT intermodulation distortion using the nonlinear discrete convolution model”, in *IEEE MTT-S, International Microwave Symposium, 2002.*

[3] A.Raffo, A.Santarelli, P.A.Traverso, M.Pagani, F.Palomba, F.Scappaviva, G.Vannini, F.Filicori “Improvement of PHEMT Intermodulation Prediction Through the Accurate Modeling of Low-Frequency Dispersion Effects”, in *IEEE MTT-S, International Microwave Symposium*, Long Beach, California, USA, June 12-17, 2005.

[4] A.Santarelli, F.Filicori, et al “A backgating model including self-heating for low-frequency dispersive effects in III-V FETs”, *Electronics Letters,* Oct 1998.

[5] W. R. Curtice, "A MESFET model for use in the design of GaAs integrated circuits," *IEEE Transactions of Microwave Theory and Techniques*, Vol. MTT-28, pp. 448-456, May 1980.

[6] High-Frequency Model Tutorial, IC-CAP 5.3.